

Influence of heat treatment modes on the structure and mechanical properties of wrought VTI-4 alloy based on orthorhombic titanium aluminide

Vitaly S. Sokolovsky^{*1,3}, PhD (Engineering), researcher at the Laboratory of Bulk Nanostructured Materials
Stanislav V. Naumov^{1,4}, PhD (Engineering), senior researcher at the Laboratory of Bulk Nanostructured Materials
Dmitry O. Panov^{1,5}, PhD (Engineering), senior researcher at the Laboratory of Bulk Nanostructured Materials
Vasily V. Lukianov^{2,6}, PhD (Engineering), Head of the Complex-Shape Forming Department
Gennady A. Salishchev^{1,7}, Doctor of Sciences (Engineering),
Head of the Laboratory of Bulk Nanostructured Materials

¹Belgorod National Research University, Belgorod (Russia)

²Scientific and Production Association “Technopark of Aviation Technologies”, Ufa (Russia)

*E-mail: sokolovskiy@bsuedu.ru

³ORCID: <https://orcid.org/0000-0002-4363-3604>

⁴ORCID: <https://orcid.org/0000-0002-4084-8861>

⁵ORCID: <https://orcid.org/0000-0002-8971-1268>

⁶ORCID: <https://orcid.org/0009-0006-3621-3966>

⁷ORCID: <https://orcid.org/0000-0002-0815-3525>

Received 09.09.2025

Revised 23.01.2026

Accepted 19.02.2026

Abstract: Problem. Currently, in the field of research on alloys based on orthorhombic Ti₂AlNb aluminide, there are no data on the relationship between heat treatment modes, structural parameters, and mechanical characteristics to ensure a balance of strength and ductility. **Aim.** To establish the relationship between heat treatment modes, microstructural characteristics (O-phase sizes, α₂-phase volume fraction) and mechanical characteristics at room temperature, as well as to determine the heat treatment mode that provides the best balance of strength and ductility for the VTI-4 alloy. **Methods.** In this work, the method of isothermal multidirectional forging was applied to form a fine-grained globular structure in order to improve the ductility characteristics of the alloy. Subsequent two-stage heat treatment was carried out in the α₂+β+O-phase region. Mechanical characteristics were determined by tensile testing. **Results.** The influence of quenching and aging temperature on the size and volume fraction of α₂ and O-phase particles was investigated. The choice of heat treatment modes aimed at forming a structure that ensures high strength and ductility properties of the VTI-4 alloy is substantiated. It was established that when heating for quenching to T=900 °C, O-phase precipitates are retained at triple junctions along β-grain boundaries; during subsequent aging, O-phase particles and interlayers are formed, the thickness of which increases with rising temperature, leading to a decrease in strength and ductility. It was also established that heating for quenching from the upper part of the α₂+β+O-phase region (T=960 °C) preserves the globular microstructure, leading to the dissolution of O-phase particles and, accordingly, saturating the β-phase with alloying elements. Increasing the quenching temperature also reduces the volume fraction of α₂-phase particles and prevents the formation of O-phase interlayers along β-grain boundaries during aging in the temperature range of 760–800 °C. **Conclusions.** The study of the influence of aging temperature in the range of 760–840 °C revealed that the lower the temperature, the smaller the thickness of O-phase particles, the higher the strength, and the lower the ductility. The optimal heat treatment mode was determined: quenching at T=960 °C for τ=2 h and aging at T=800 °C for τ=6 h. After such heat treatment, the wrought VTI-4 alloy demonstrates high strength and ductility (σ_{0.2}=1180 MPa, σ_U=1300 MPa, δ=6.2 %).

Keywords: orthorhombic titanium aluminide Ti₂NbAl; VTI-4 alloy; isothermal multidirectional forging; quenching; aging; mechanical properties

Acknowledgments: This work was financially supported by the Russian Science Foundation (agreement No. 19-79-30066) using the equipment of the Common Use Center “Technologies and Materials” of the National Research University “BelSU”, https://rscf.ru/prjcard_int?19-79-30066.

The paper was written on the reports of the participants of the XII International School of Physical Materials Science (SPM-2025), Togliatti, September 15–19, 2025.

For citation: Sokolovsky V.S., Naumov S.V., Panov D.O., Lukianov V.V., Salishchev G.A. Influence of Heat Treatment Modes on the Structure and Mechanical Properties of Wrought VTI-4 Alloy Based on Orthorhombic Titanium Aluminide. *Frontier Materials & Technologies*, 2026, no. 1, pp. 97–106. DOI: <https://doi.org/10.18323/2782-4039-2026-1-75-8>.

© Sokolovsky V.S., Naumov S.V., Panov D.O.,
Lukianov V.V., Salishchev G.A., 2026

INTRODUCTION

Alloys based on orthorhombic Ti_2AlNb aluminide, including the domestic VTI-4 alloy, are attracting increasing attention due to their low density, high specific strength, enhanced heat resistance, and fire safety [1–3]. These properties make them promising for applications in compressor and turbine components of aircraft engines, as well as in ground-based power plants operating at temperatures of 600–750 °C [4; 5]. At the same time, these alloys are multiphase, and consequently, their mechanical characteristics depend on the size and volume fractions of the phases [5; 6].

The phase composition of the alloys (β -, α -, and O-phases) varies depending on the heating temperature. Control over the quantity of phases, their ratio, crystal structure, and degree of ordering is achieved through alloying and processing regimes [7–9]. Recent studies emphasize the importance of controlling the size, morphology, and distribution of phases to achieve an optimal balance of strength, ductility, and heat resistance in Ti_2AlNb -based orthorhombic aluminide alloys [7; 10].

In addition to classical heat treatments, approaches to processing such alloys include thermomechanical treatment with large plastic deformations. For example, the application of extrusion resulted in increased strength and ductility due to structure refinement [11]. Multidirectional forging has proven to be an equally effective method for refining the coarse-grained structure of cast alloys, and subsequent quenching and aging lead to the formation of dispersed O-phase precipitates, significantly enhancing strength characteristics [6; 12; 13].

Hot forging or rolling significantly refine the structure, causing a simultaneous increase in ductility and strength [5]. Subsequent heat treatment, consisting of quenching and aging, is the most effective way to obtain a balanced set of properties in these alloys. The choice of quenching temperature determines the α_2 -phase volume fraction and the degree of β -phase supersaturation after quenching; varying the aging regimes allows control over the dispersion of O-phase particles and, consequently, the mechanical properties [5; 7; 10].

Hot deformation and subsequent heat treatment promote a uniform α_2 -phase distribution and an increase in

ductility [4]. Heat treatment of VTI-4 alloy welded joints increases ductility; according to the authors, this was associated with an increase in the uniformity of phase distribution [14]. Despite the research conducted, a number of unresolved tasks remain. The key among them is the determination of processing regimes and parameters of the forming structure that can ensure both high strength and tensile ductility of the alloy.

The aim of this work is to establish the relationship between heat treatment modes, microstructural characteristics (O-phase sizes, α_2 -phase volume fraction) and mechanical characteristics at room temperature, as well as to determine the heat treatment mode that provides the best balance of strength and ductility for the VTI-4 alloy.

METHODS

Material of investigation

The material under investigation was VTI-4 alloy produced by remelting according to the “vacuum arc remelting – skull melting – vacuum arc remelting” scheme. Alloy workpieces were cut and subjected to pack rolling at a temperature of 1060 ± 10 °C, which corresponded to the $\alpha_2 + \beta$ -phase region. The hot-rolled plate was used in this work as the initial state.

Isothermal multidirectional forging

Workpieces with dimensions of $40 \times 30 \times 60$ mm³ were cut from the plate using a VL400Q / VL600Q electrical discharge machine (Sodick, China). The workpieces were heated to $T = 950$ °C in an N 321 mod. 400v3/N/PE chamber furnace (Nabertherm, Germany) and held for 30 minutes. At a temperature of 950 °C, which corresponded to the upper part of the $\alpha_2 + \beta + O$ -phase region, the workpieces were deformed with an accumulated strain of 750 % using a DEVR 1000 hydraulic press (Gidropress, Russia) equipped with a Miterm-T3 muffle furnace (Microinstrument, Russia). Deformation was carried out at a strain rate of 5 mm/min with a strain of 50 % per pass in each direction (Fig. 1). After each pass, the workpiece was rotated by 90°. The accumulated total strain was $\epsilon_{\Sigma} = 300$ %. The obtained workpiece was cooled in still air.

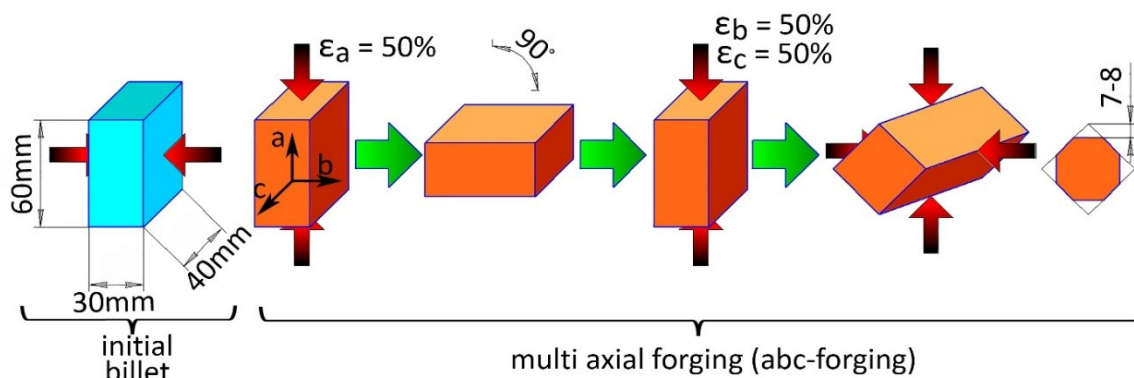


Fig. 1. Schematic diagram of the isothermal multidirectional forging process

Рис. 1. Схема проведения всесторонней изотермическойковки

Heat treatment

Plates with dimensions of 25×12×2.5 mm were cut from the obtained workpieces and subjected to heat treatment in an LT 5/12/P320 muffle furnace (Nabertherm, Germany). The quenching temperature is determined by the fact that heating to the β - or $\alpha_2+\beta$ -phase regions leads to an increase in β -grain sizes, which deteriorates the material's characteristics. At the same time, when heating in the upper and middle parts of the $\alpha_2+\beta+O$ -phase region, almost complete dissolution of the O-phase occurs, which allows the $\beta \rightarrow O$ transformation to occur during subsequent aging. The holding time at the quenching temperature was 2 hours. This is related to the slow kinetics of O-phase dissolution during heating in the $\alpha_2+\beta+O$ -phase region. The workpieces were subjected to two-stage heat treatment according to the following regimes:

1) heating to $T_1=900\text{ }^\circ\text{C}$ ($\alpha_2+\beta+O$ -phase region), holding for 2 hours, water quenching, followed by aging for 6 hours at temperatures $T_2=760\text{ }^\circ\text{C}$ ($\beta+O$ -phase region), $T_2=800\text{ }^\circ\text{C}$, and $T_2=840\text{ }^\circ\text{C}$ ($\alpha_2+\beta+O$ -phase region) with furnace cooling;

2) heating to temperature $T_1=960\text{ }^\circ\text{C}$ (upper part of the $\alpha_2+\beta+O$ -phase region), holding for 2 hours, then water quenching. After this, aging is carried out at temperatures $T_2=760\text{ }^\circ\text{C}$ ($\beta+O$ -phase region), $T_2=800\text{ }^\circ\text{C}$, and $T_2=840\text{ }^\circ\text{C}$ ($\alpha_2+\beta+O$ -phase region). Cooling is carried out using the furnace.

Mechanical testing

Flat specimens for mechanical testing with a gauge section cross-section of 3×1.5 mm were cut from the plates. They were subjected to mechanical grinding using abrasive paper with stepwise reduction in grit size, and then polishing using polishing cloth and OP-S colloidal silica suspension (Struers, Switzerland). Mechanical grinding and polishing were carried out on a Struers LaboPol-5 grinding and polishing machine (Struers, Switzerland). Tensile tests were performed on an Instron 5882 universal testing machine (USA) at a deformation rate of 0.36 mm/min. The elongation of the specimens was measured on an Olympus STM6 tool microscope (Japan) based on the distance between marks applied to the edges of the gauge section before testing. Percentage elongation was calculated as the ratio of the gauge section length after testing to the initial gauge section length, multiplied by 100 %. Mechanical properties were determined on an Instron 5882 testing machine (Instron, USA) using 3 specimens per condition.

Structure investigation

To study the microstructure of the alloy, a Quanta 600 scanning electron microscope (SEM) (FEI, USA) with a LaB6 cathode was used. Imaging was carried out in electron backscattered diffraction (EBSD) contrast mode at an accelerating voltage of 30 kV. Samples for SEM investigation were prepared by careful mechanical grinding and polishing, similar to the method of sample preparation for tensile testing. To study the microstructure of the hot-rolled plate, the method of constructing orientation maps using electron backscatter diffraction (EBSD) was applied.

The maps were constructed using a Nova Nano SEM 450 scanning electron microscope (FEI, USA) equipped with a Hikari EBSD detector (EDAX, USA). Samples were prepared by electropolishing after preliminary mechanical grinding and polishing. Electropolishing was carried out in a mixture of 5 % perchloric acid, 35 % butanol, and 60 % methanol at a voltage of 27 V and $-32\text{ }^\circ\text{C}$ using a LectroPol-5 device (Struers, Denmark).

Data processing

Grain and particle sizes were determined by the intersection method in accordance with GOST R ISO 643–2011. The volume fraction of phase particles in the alloy structure was calculated by measuring the areas and determining their ratios. The volume fraction of phase particles was determined as the ratio of the sums of the areas occupied by individual phase particles to the total area of the image. Five different fields of view were used for analysis. The areas of individual phases were determined using Digimizer software version 4.3.0 (MedCalc Software).

RESULTS

The microstructure of the VTI-4 alloy in the initial hot-rolled state consists of β -grains elongated along the rolling direction with average dimensions of 400×90 μm , respectively (Fig. 2 a, b). Along the β -grain boundaries, chains of individual α_2 -phase particles are located, with a volume fraction of 6±1 % and a size of 3.2±0.4 μm (Fig. 2 b).

The application of isothermal multidirectional forging in the upper part of the $\alpha_2+\beta+O$ -phase region at $T=950\text{ }^\circ\text{C}$ made it possible to significantly refine the structure. The size of β -grains decreased to 7 μm , and the fraction of α_2 -phase particles increased to 15.1 % with an average size of 1.9 μm (Fig. 3; Table 1). Furthermore, O-phase precipitates ($\approx 2\text{ }^\circ\mu\text{m}$) are visible along the boundaries and within the body of β -grains, as well as at triple junctions of β -grains/ α_2 -phase particles (Fig. 3).

In the microstructure of the VTI-4 alloy quenched from $T=900\text{ }^\circ\text{C}$ after aging at $T=760, 800, \text{ and } 840\text{ }^\circ\text{C}$, acicular O-phase particles precipitate within the β -phase grains, and O-phase interlayers form along the β -grain boundaries (Fig. 4). The lower the aging temperature, the smaller the thickness of the O-phase particles and interlayers (Table 1, Fig. 4). The volume fraction of α_2 -phase particles did not depend on the aging temperature and amounted to 5.4±0.2 %, with their size being 2.2±0.3 μm .

The microstructure of the VTI-4 alloy after forging, quenching at $T=960\text{ }^\circ\text{C}$, and subsequent aging is characterized by the absence of O-phase interlayers along the β -phase grain boundaries after aging at 760 and 800 $^\circ\text{C}$ (Table 1, Fig. 5). Clearly, the lower the aging temperature, the smaller the thickness of the O-phase particles (Table 1). The volume fraction of α_2 -phase particles is 3.1±0.5 %, and their size is 3.3±0.5 μm across the entire investigated range of aging temperatures.

After isothermal multidirectional forging, the alloy demonstrates a rather low level of percentage elongation of 2.1±0.1 % and a high ultimate tensile strength of 1273±10 MPa (Table 2). After quenching at $T=900\text{ }^\circ\text{C}$,

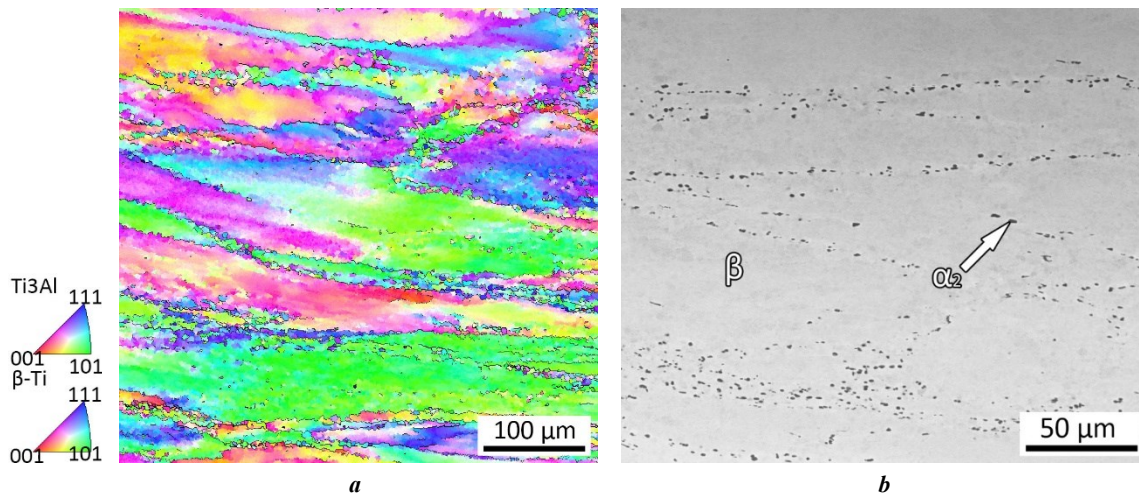


Fig. 2. Microstructure of the VTi-4 alloy in the initial hot-rolled state, rolling direction oriented horizontally: **a** – EBSD; **b** – SEM. Arrows indicate α_2 -phase particles
Рис. 2. Микроструктура сплава ВТИ-4 в исходном горячекатанном состоянии, направление прокатки ориентировано горизонтально: **a** – ДОРЭ; **b** – СЭМ. Стрелками обозначены частицы α_2 -фазы

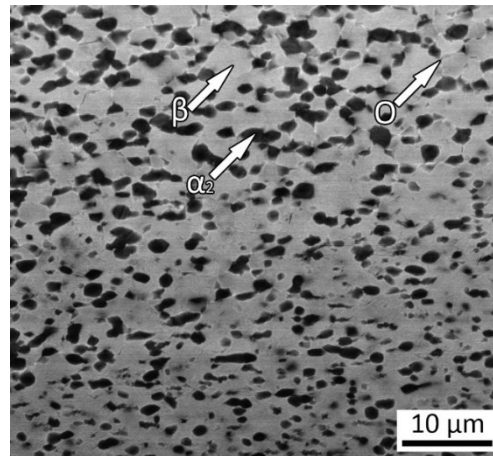


Рис. 3. Микроструктура сплава ВТИ-4 после всесторонней изотермическойковки. Стрелками обозначены зерна/частицы β -, O- и α_2 -фаз

the achieved strength level is maintained, and the percentage elongation increases by almost an order of magnitude to 18.9 ± 0.3 %. An increase in the aging temperature slightly reduces the ultimate tensile strength and leads to some decrease in percentage elongation to 14.9 ± 0.6 % (Table 2). Increasing the quenching temperature to $T=960$ °C and aging at $T=760$ °C leads to some increase in strength and ductility compared to the forged state (Table 1). With an increase in the aging temperature to 800 °C, an almost twofold increase in percentage elongation to 6.2 % is observed, while the ultimate tensile strength is maintained at 1300 MPa (Table 2). A further increase in the aging temperature to 840 °C significantly reduces the ultimate tensile strength to 1190 MPa and leads to an increase in percentage elongation to 12.6 %.

DISCUSSION

The results confirm that isothermal multidirectional forging in the $\alpha_2 + \beta + O$ region effectively refines the structure due to the development of dynamic recrystallization, forming a globular structure that is stable during heat treatment (Fig. 3). The choice of quenching temperature determines the degree of supersaturation of the β -phase with alloying elements at the temperature of the cooling medium and, consequently, the O-phase formation during aging. When heating for quenching to $T=900$ °C, O-phase precipitates present in the initial state after forging are retained at triple junctions, and interlayers form along the β -grain boundaries, which obviously adversely affect the ductility characteristics of the alloy (Figs. 4, 5). During subsequent aging over

Table 1. Microstructural parameters of VTI-4 alloy after heat treatment
Таблица 1. Микроструктурные параметры сплава ВТИ-4 термической обработки

Heat treatment mode	β -phase grain size, μm	α_2 -phase particles		O-phase particles		O-phase interlayer thickness, μm
		Size, μm	Volume fraction, %	Length, μm	Thickness, μm	
Forging	7 ± 2	1.9 ± 0.3	15.1 ± 4.2	2.0 ± 0.2	0.31 ± 0.23	0.0 ± 0.0
$T_1=900\text{ }^\circ\text{C}; T_2=760\text{ }^\circ\text{C}$	7 ± 2	2.2 ± 0.3	5.4 ± 0.2	2.1 ± 0.1	0.31 ± 0.21	1.2 ± 0.2
$T_1=900\text{ }^\circ\text{C}; T_2=800\text{ }^\circ\text{C}$				2.2 ± 0.1	0.35 ± 0.27	1.8 ± 0.3
$T_1=900\text{ }^\circ\text{C}; T_2=840\text{ }^\circ\text{C}$				2.3 ± 0.1	0.40 ± 0.32	2.4 ± 0.6
$T_1=960\text{ }^\circ\text{C}; T_2=760\text{ }^\circ\text{C}$		3.3 ± 0.5	3.1 ± 0.5	2.1 ± 0.1	0.12 ± 0.04	0.0 ± 0.0
$T_1=960\text{ }^\circ\text{C}; T_2=800\text{ }^\circ\text{C}$				2.2 ± 0.1	0.19 ± 0.05	0.0 ± 0.0
$T_1=960\text{ }^\circ\text{C}; T_2=840\text{ }^\circ\text{C}$				2.3 ± 0.1	0.28 ± 0.02	1.1 ± 0.2

Note. T_1 – quenching temperature, T_2 – aging temperature.

Holding time at quenching temperature is 2 hours, at aging temperature – 6 hours.

Примечание. T_1 – температура закалки; T_2 – температура старения.

Выдержка при температуре закалки 2 часа, а при температуре старения 6 часов.

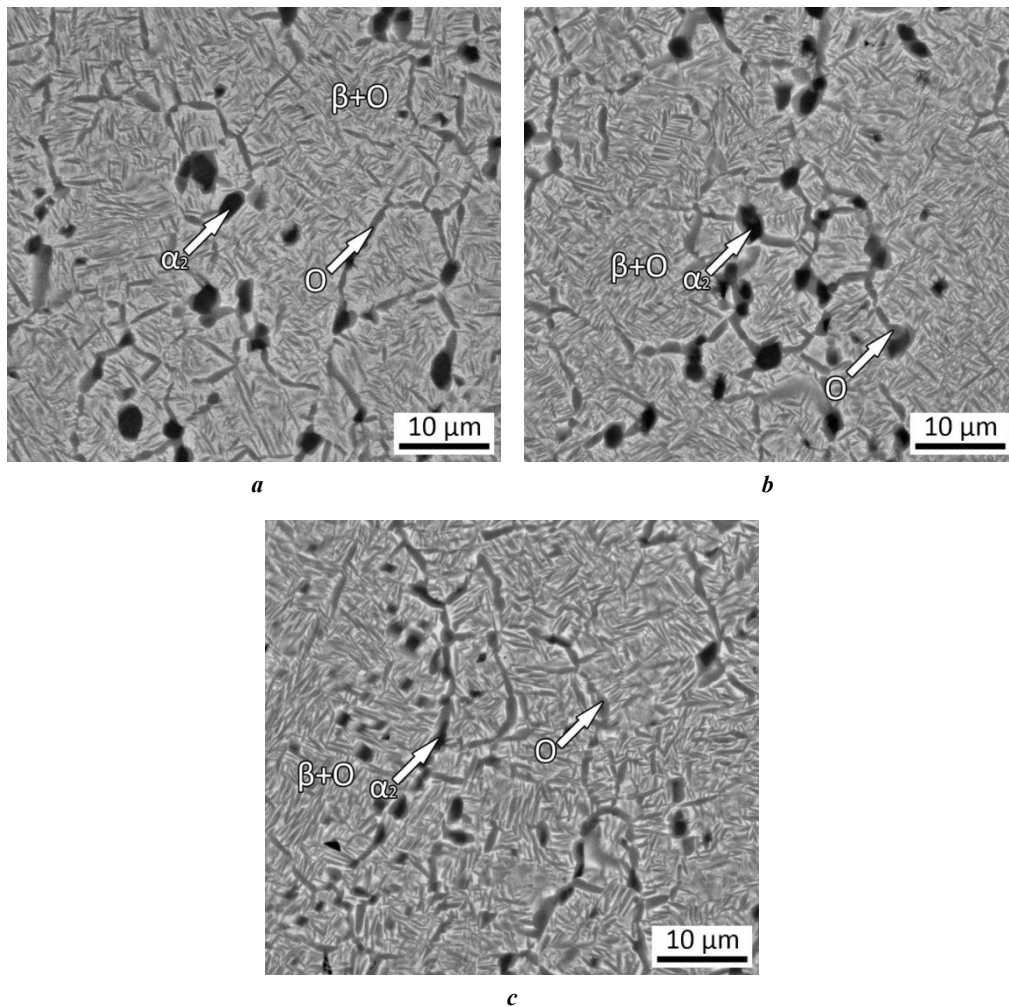


Fig. 4. Microstructure of the VTI-4 alloy after quenching at $T=900\text{ }^\circ\text{C}$ and subsequent aging
а – at $T=760\text{ }^\circ\text{C}$; **б** – $T=800\text{ }^\circ\text{C}$; **с** – $T=840\text{ }^\circ\text{C}$. Arrows indicate particles of O and α_2 phases
Рис. 4. Микроструктура сплава ВТИ-4 после закалки с $T=900\text{ }^\circ\text{C}$ и последующего старения
а – при $T=760\text{ }^\circ\text{C}$; **б** – $T=800\text{ }^\circ\text{C}$; **с** – $T=840\text{ }^\circ\text{C}$. Стрелками обозначены частицы O- и α_2 -фаз

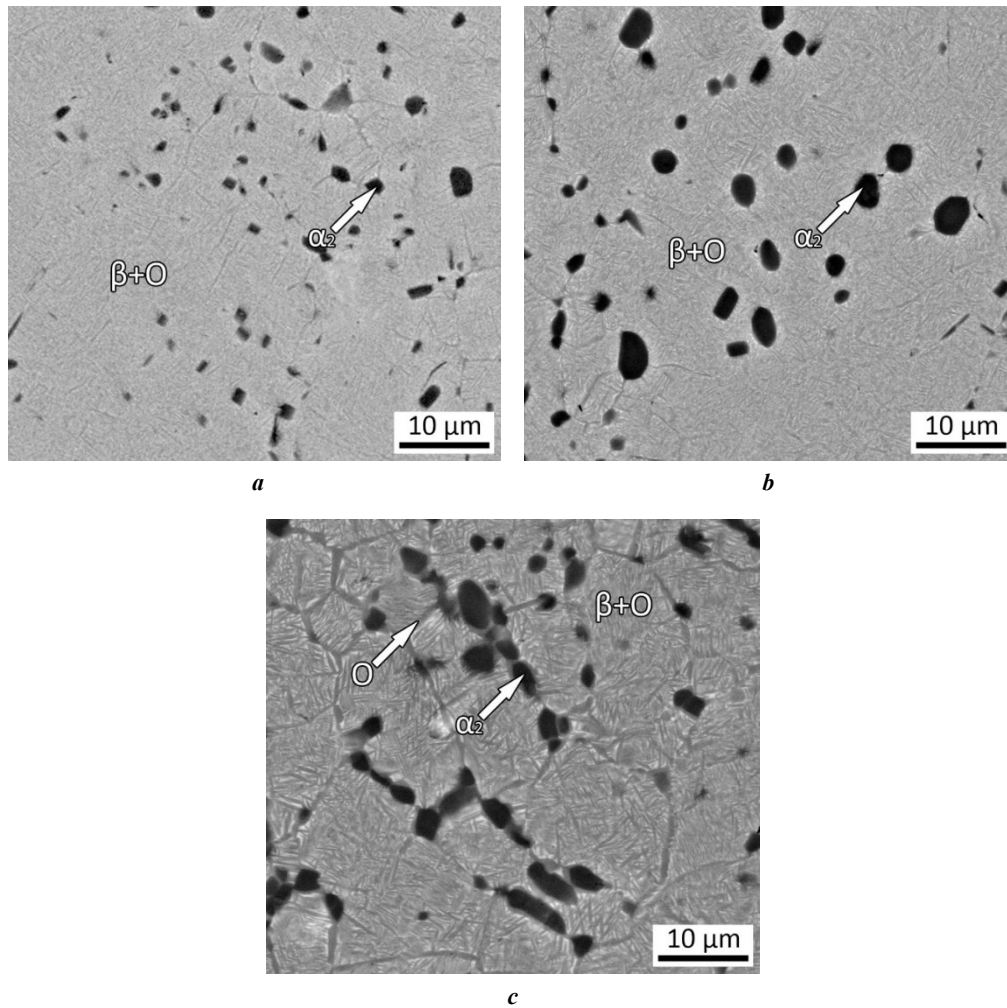


Fig. 5. Microstructure of the VTI-4 alloy after quenching at $T=960\text{ }^{\circ}\text{C}$ and subsequent aging *a* – at $T=760\text{ }^{\circ}\text{C}$; *b* – $T=800\text{ }^{\circ}\text{C}$; *c* – $T=840\text{ }^{\circ}\text{C}$. Arrows indicate particles of *O* and α_2 phases
Рис. 5. Микроструктура сплава ВТИ-4 после закалки с $T=960\text{ }^{\circ}\text{C}$ и последующего старения при *a* – при $T=760\text{ }^{\circ}\text{C}$; *b* – $T=800\text{ }^{\circ}\text{C}$; *c* – $T=840\text{ }^{\circ}\text{C}$. Стрелками обозначены частицы *O*- и α_2 -фаз

Table 2. Mechanical properties of the VTI-4 alloy after forging and heat treatment
Таблица 2. Механические свойства сплава ВТИ-4 послековки и термической обработки

Tensile	Forging	$T_1=900\text{ }^{\circ}\text{C}$			$T_1=960\text{ }^{\circ}\text{C}$		
		$T_2=760\text{ }^{\circ}\text{C}$	$T_2=800\text{ }^{\circ}\text{C}$	$T_2=840\text{ }^{\circ}\text{C}$	$T_2=760\text{ }^{\circ}\text{C}$	$T_2=800\text{ }^{\circ}\text{C}$	$T_2=840\text{ }^{\circ}\text{C}$
σ_B , МПа	1273±10	1276±12	1186±8	1146±14	1314±9	1300±11	1190±15
δ , %	2.1±0.1	18.9±0.3	17.1±0.4	14.9±0.6	3.4±0.3	6.2±0.2	12.6±0.6

Note. T_1 – температура закалки, T_2 – температура старения.
 Примечание. T_1 – quenching temperature, T_2 – aging temperature.

the entire investigated temperature range ($T=760\text{--}840\text{ }^{\circ}\text{C}$), the thickness of the interlayers and *O*-phase particles within the β -grains increases with increasing aging temperature, reducing strength and ductility (Table 2), which was also noted with increasing aging temperature [4; 5; 9]. Heating for quenching to $T=960\text{ }^{\circ}\text{C}$ leads to almost complete *O*-phase dissolution, freeing the grain boundaries from interlayers (Fig. 5). At the same

time, the grain size is preserved, which can contribute to obtaining more balanced properties of both strength and ductility (Table 2). During aging in the $\beta+O$ -phase region ($T=760\text{ }^{\circ}\text{C}$), dispersed *O*-phase particles are formed, which increase strength [2; 9]. With an increase in aging temperature and transition to the $\alpha_2+\beta+O$ -phase region ($T=800\text{ }^{\circ}\text{C}$), the percentage elongation increases twofold, and strength decreases, which is associated with

Table 3. Mechanical properties of Ti₂AlNb-based alloys
Таблица 3. Механические свойства сплавов на основе Ti₂AlNb

Alloy, at. %	σ_b , MPa	δ , %
Ti-23.0Al-23.0Nb-1.3V-0.8Zr-0.5Mo-0.3Si (VTI-4) [*]	1300±11	6.2±0.2
Ti-22.0Al-24.0Nb-1.5Zr-1.5Mo-0.8Ta-0.6W-0.4Si (VIT1) [5]	1260±30	5.8±0.3
Ti-22Al-25Nb [15]	927±8	6.9±0.9
Ti-22Al-25Nb (rolled) [15]	1169±10	25.7±0.6
Ti-22Al-23Nb-1Mo-1Zr [11]	1225±20	6.3±0.2
Ti-20.3Al-24.7Nb [16]	1541±40	1.75±0.4
Ti-22Al-25Nb [10]	1145±50	10.0±0.2

Note. *Results of the present study.

Примечание. *Результаты данного исследования.

an increase in the thickness of the O-phase particles. After aging at T=840 °C, the formation of O-phase interlayers along the β -grain boundaries was detected (Figs. 4, 5), which caused a drop in strength and is consistent with data from other authors [9]. Thus, quenching at T=960 °C and aging at T=800 °C make it possible to avoid the formation of undesirable O-phase interlayers and also to precipitate dispersed O-phase particles within the β -grains, which together provide balanced mechanical characteristics.

The results of the work show that isothermal multidirectional forging (T=950 °C) of the hot-rolled VTI-4 alloy, water quenching from the upper part of the α_2 + β +O-phase region (T=960 °C), and subsequent aging in the same phase region at T=800 °C make it possible to obtain a structure providing a balanced level of strength (σ_U =1300±11 MPa) and ductility (δ =6.2±0.2%) (Table 2).

A comparison of the combination of strength and ductility characteristics obtained in this work with known results obtained on other Ti₂AlNb-based alloys (Table 3) shows that the use of isothermal multidirectional forging and subsequent two-stage treatment allows achieving a higher combination of strength and ductility. In particular, a rolled Ti-20.3Al-24.7Nb alloy demonstrates higher strength (1541±40 MPa), but its ductility is three times lower (1.75±0.4 %) [16]. The closest strength properties (σ_U =1260±30 MPa) and ductility (δ =5.8±0.3 %) were shown by the VIT1 alloy subjected to thermomechanical treatment [5].

As shown by the authors of [15], additional structure refinement during thermomechanical treatment made it possible to increase the ultimate tensile strength by more than 250 MPa and the percentage elongation by 19 % (Table 3), which caused the overall increase in properties. In work [5], optimal properties were achieved with an O-phase particle thickness of 0.12 μ m and an α_2 -phase fraction of 3 %. In our case, for the regime providing σ_U =1300±11 MPa and δ =6.2±0.2 %, the thickness was 0.19 μ m and the α_2 -phase fraction was 3 % (Table 1), which falls within the same range and confirms the established pattern. Studies of the VIT1 alloy showed similar properties

(σ_U =1260±30 MPa, δ =5.8±0.3 %) after aging at 850 °C [5], which is close to the results of this work. At the same time, according to the data of work [5], the thickness of O-phase particles in the VIT1 alloy was 0.07 μ m smaller than in our study. This difference may be explained by the inhibiting effect of molybdenum in the composition of VIT1 on diffusion and particle growth, which is confirmed by data in the scientific literature [17].

CONCLUSIONS

1. It has been established that increasing the quenching temperature from 900 to 960 °C reduces the α_2 -phase fraction from 5 to 3%, suppresses the formation of O-phase interlayers along β -grain boundaries during aging in the range of T=760–800 °C, and refines the O-phase particles within β -grains from 0.35 to 0.19 μ m, leading to an increase in ultimate tensile strength from 1186±8 to 1300±11 MPa.

2. It has been established that refining β -grains to 7 μ m by isothermal multidirectional forging, followed by a two-stage heat treatment designed to produce a structure with an α_2 -phase fraction of 3 % and an O-phase particle thickness of 0.19 μ m, provides a high combination of strength and ductility in the VTI-4 alloy (σ_U =1300±11 MPa, δ =6.2±0.2 %). The optimal heat treatment regimes for the wrought VTI-4 alloy are the following: holding for 2 h at T=960 °C, water quenching, and aging for 6 h at T=800 °C.

REFERENCES

- Banerjee D. The intermetallic Ti₂AlNb. *Progress in Materials Science*, 1997, vol. 42, no. 1-4, pp. 135–158. DOI: [10.1016/S0079-6425\(97\)00012-1](https://doi.org/10.1016/S0079-6425(97)00012-1).
- Goyal K., Sardana N. Mechanical Properties of the Ti₂AlNb Intermetallic: A Review. *Transactions of the Indian Institute of Metals*, 2021, vol. 74, no. 8, pp. 1839–1853. DOI: [10.1007/s12666-021-02307-5](https://doi.org/10.1007/s12666-021-02307-5).
- Goyal K., Bera C., Sardana N. Temperature-dependent structural, mechanical, and thermodynamic properties of B2-phase Ti₂AlNb for aerospace applications. *Journal*

- of *Materials Science*, 2022, vol. 57, pp. 19553–19570. DOI: [10.1007/s10853-022-07788-3](https://doi.org/10.1007/s10853-022-07788-3).
4. Illarionov A.G., Stepanov S.I., Naschetnikova I.A., Popov A.A., Popov A.A., Soundappan P., Thulasi Raman K.H., Suwas S. A Review-Additive Manufacturing of Intermetallic Alloys Based on Orthorhombic Titanium Aluminide Ti₂AlNb. *Materials*, 2023, vol. 16, no. 3, article number 991. DOI: [10.3390/ma16030991](https://doi.org/10.3390/ma16030991).
 5. Sokolovskiy V.S., Nozdracheva E.I., Kyaramyan K.A., Bykov Yu.G., Alekseev E.B., Salishchev G.A. Effect of hot deformation and heat treatment conditions on the structure and mechanical properties of the vit1 alloy based on orthorhombic titanium aluminide. *Izvestiya. Non-Ferrous Metallurgy*, 2025, vol. 31, no. 1, pp. 67–79. EDN: [JKGFPM](https://www.edn.net/JKGFPM).
 6. Caihong Jing, Shoujiang Qu, Aihan Feng, Hao Wang, Daolun Chen. Influence of Microstructure and Texture on Tensile Properties of an As-Rolled Ti₂AlNb-Based Alloy. *Metals*, 2023, vol. 13, no. 6, article number 631. DOI: [10.3390/met13060631](https://doi.org/10.3390/met13060631).
 7. Tianze Liu, Xuwen Li, Boxin Wei. The Influences of Heat Treatment on the Microstructure and Mechanical Properties of Rolled Ti₂AlNb. *Metals*, 2023, vol. 13, no. 5, article number 886. DOI: [10.3390/met13050886](https://doi.org/10.3390/met13050886).
 8. Chirumamilla A., Gautam G.S. Effect of alloying additions on the lattice ordering of Ti₂AlNb intermetallic. *Journal of Materials Research*, 2026, vol. 41, pp. 169–179. DOI: [10.1557/s43578-025-01684-7](https://doi.org/10.1557/s43578-025-01684-7).
 9. Illarionov A.G., Demakov S.L., Vodolazskiy F.V., Stepanov S.I., Illarionova S.M., Shabanov M.A., Popov A.A. Alloys based on orthorhombic intermetallic: phase composition, alloying, structure, properties. *Metallurgist*, 2023, vol. 67, pp. 305–323. DOI: [10.1007/s11015-023-01518-z](https://doi.org/10.1007/s11015-023-01518-z).
 10. Lin Yang, Zhiqiang Bu, Jinfu Li. Microstructure and mechanical properties of as-cast Ti₂AlNb alloys. *Materials & Design*, 2025, vol. 254, article number 114138. DOI: [10.1016/j.matdes.2025.114138](https://doi.org/10.1016/j.matdes.2025.114138).
 11. Shishuang Liu, Jingxia Cao, Yi Zhou, Chenrui Hou, Shenglong Dai, Xu Huang. Microstructure evolution and mechanical properties of a high-strength Ti₂AlNb alloy processed by large-strain two-pass hot extrusion. *Journal of Alloys and Compounds*, 2022, vol. 925, article number 166715. DOI: [10.1016/j.jallcom.2022.166715](https://doi.org/10.1016/j.jallcom.2022.166715).
 12. Yinling Zhang, Aihan Feng, Shoujiang Qu, Jun Shen, Daolun Chen. Microstructure and low cycle fatigue of a Ti₂AlNb-based lightweight alloy. *Journal of Materials Science & Technology*, 2020, vol. 44, pp. 140–147. DOI: [10.1016/j.jmst.2020.01.032](https://doi.org/10.1016/j.jmst.2020.01.032).
 13. Panov D.O., Naumov S.V., Stepanov N.D., Sokolovsky V.S., Volokitina E., Kashaev N., Ventzke V., Dinse R., Riekehr S., Povolyaeva E., Nochovnaya N., Alekseev E., Zhrebtsov S., Salishchev G. Effect of pre-heating and post-weld heat treatment on structure and mechanical properties of laser beam-welded Ti₂AlNb-based joints. *Intermetallics*, 2022, vol. 143, article number 107466. DOI: [10.1016/j.intermet.2022.107466](https://doi.org/10.1016/j.intermet.2022.107466).
 14. Naumov S.V., Panov D.O., Chernichenko R.S., Sokolovskiy V.S., Volokitina E.I., Stepanov N.D., Zhrebtsov S.V., Alekseev E.B., Nochovnaya N.A., Salishchev G.A. Structure and mechanical properties of welded joints from alloy based on VTI-4 orthorhombic titanium aluminide produced by pulse laser welding. *Izvestiya. Non-Ferrous Metallurgy*, 2023, vol. 29, no. 2, pp. 57–73. DOI: [10.17073/0021-3438-2023-2-57-73](https://doi.org/10.17073/0021-3438-2023-2-57-73).
 15. Shengwei Zhang, Mingzhe Xi, Rui Liu, Mingyue Li, Xiaotian Guo, Yiming Gui, Jing Wu. Fabricating Ti–22Al–25Nb Intermetallic with Ductility Higher than 25% by Advanced Printing Technique: Point-Forging and Laser-Deposition. *Materials Science and Engineering: A*, 2022, vol. 850, article number 143520. DOI: [10.1016/j.msea.2022.143520](https://doi.org/10.1016/j.msea.2022.143520).
 16. Xiaochong Sui, Guofeng Wang, Qing Liu, Yongkang Liu, Yuqing Chen. Fabricating Ti₂AlNb sheet with tensile strength higher than 1500 MPa by hot packed rolling spark-plasma-sintered pre-alloyed Ti the B2 + O phase field. *Journal of Alloys and Compounds*, 2021, vol. 876, article number 160110. DOI: [10.1016/j.jallcom.2021.160110](https://doi.org/10.1016/j.jallcom.2021.160110).
 17. Yaran Zhang, Yongchang Liu, Liming Yu, Hongyan Liang, Yuan Huang, Zongqing Ma. Microstructures and tensile properties of Ti₂AlNb and Mo-modified Ti₂AlNb alloys fabricated by hot isostatic pressing. *Materials Science and Engineering: A*, 2020, vol. 776, article number 139043. DOI: [10.1016/j.msea.2020.139043](https://doi.org/10.1016/j.msea.2020.139043).

СПИСОК ЛИТЕРАТУРЫ

1. Banerjee D. The intermetallic Ti₂AlNb // *Progress in Materials Science*. 1997. Vol. 42. № 1–4. P. 135–158. DOI: [10.1016/S0079-6425\(97\)00012-1](https://doi.org/10.1016/S0079-6425(97)00012-1).
2. Goyal K., Sardana N. Mechanical Properties of the Ti₂AlNb Intermetallic: A Review // *Transactions of the Indian Institute of Metals*. 2021. Vol. 74. № 8. P. 1839–1853. DOI: [10.1007/s12666-021-02307-5](https://doi.org/10.1007/s12666-021-02307-5).
3. Goyal K., Bera C., Sardana N. Temperature-dependent structural, mechanical, and thermodynamic properties of B2-phase Ti₂AlNb for aerospace applications // *Journal of Materials Science*. 2022. Vol. 57. P. 19553–19570. DOI: [10.1007/s10853-022-07788-3](https://doi.org/10.1007/s10853-022-07788-3).
4. Illarionov A.G., Stepanov S.I., Naschetnikova I.A., Popov A.A., Popov A.A., Soundappan P., Thulasi Raman K.H., Suwas S. A Review-Additive Manufacturing of Intermetallic Alloys Based on Orthorhombic Titanium Aluminide Ti₂AlNb // *Materials*. 2023. Vol. 16. № 3. Article number 991. DOI: [10.3390/ma16030991](https://doi.org/10.3390/ma16030991).
5. Соколовский В.С., Ноздрачева Е.И., Кярамян К.А., Быков Ю.Г., Алексеев Е.Б., Салищев Г.А. Влияние режимов горячей деформации и термической обработки на структуру и механические свойства сплава на основе орторомбического алюминиды титана ВИТ1 // *Известия высших учебных заведений. Цветная металлургия*. 2025. Т. 31. № 1. С. 67–79. EDN: [JKGFPM](https://www.edn.net/JKGFPM).
6. Caihong Jing, Shoujiang Qu, Aihan Feng, Hao Wang, Daolun Chen. Influence of Microstructure and Texture on Tensile Properties of an As-Rolled Ti₂AlNb-Based Alloy // *Metals*. 2023. Vol. 13. № 6. Article number 631. DOI: [10.3390/met13060631](https://doi.org/10.3390/met13060631).
7. Tianze Liu, Xuwen Li, Boxin Wei. The Influences of Heat Treatment on the Microstructure and Mechanical Properties of Rolled Ti₂AlNb // *Metals*. 2023. Vol. 13. № 5. Article number 886. DOI: [10.3390/met13050886](https://doi.org/10.3390/met13050886).

8. Chirumamilla A., Gautam G.S. Effect of alloying additions on the lattice ordering of Ti₂AlNb intermetallic // Journal of Materials Research. 2026. Vol. 41. P. 169–179. DOI: [10.1557/s43578-025-01684-7](https://doi.org/10.1557/s43578-025-01684-7).
9. Illarionov A.G., Demakov S.L., Vodolazskiy F.V., Stepanov S.I., Illarionova S.M., Shabanov M.A., Popov A.A. Alloys based on orthorhombic intermetallic: phase composition, alloying, structure, properties // Metallurgist. 2023. Vol. 67. P. 305–323. DOI: [10.1007/s11015-023-01518-z](https://doi.org/10.1007/s11015-023-01518-z).
10. Lin Yang, Zhiqiang Bu, Jinfu Li. Microstructure and mechanical properties of as-cast Ti₂AlNb alloys // Materials & Design. 2025. Vol. 254. Article number 114138. DOI: [10.1016/j.matdes.2025.114138](https://doi.org/10.1016/j.matdes.2025.114138).
11. Shishuang Liu, Jingxia Cao, Yi Zhou, Chenrui Hou, Shenglong Dai, Xu Huang. Microstructure evolution and mechanical properties of a high-strength Ti₂AlNb alloy processed by large-strain two-pass hot extrusion // Journal of Alloys and Compounds. 2022. Vol. 925. Article number 166715. DOI: [10.1016/j.jallcom.2022.166715](https://doi.org/10.1016/j.jallcom.2022.166715).
12. Yinling Zhang, Aihan Feng, Shoujiang Qu, Jun Shen, Daolun Chen. Microstructure and low cycle fatigue of a Ti₂AlNb-based lightweight alloy // Journal of Materials Science & Technology. 2020. Vol. 44. P. 140–147. DOI: [10.1016/j.jmst.2020.01.032](https://doi.org/10.1016/j.jmst.2020.01.032).
13. Panov D.O., Naumov S.V., Stepanov N.D., Sokolovsky V.S., Volokitina E., Kashaev N., Ventzke V., Dinse R., Riekehr S., Povolyaeva E., Nochovnaya N., Alekseev E., Zherebtsov S., Salishchev G. Effect of pre-heating and post-weld heat treatment on structure and mechanical properties of laser beam-welded Ti₂AlNb-based joints // Intermetallics. 2022. Vol. 143. Article number 107466. DOI: [10.1016/j.intermet.2022.107466](https://doi.org/10.1016/j.intermet.2022.107466).
14. Наумов С.В., Панов Д.О., Черниченко Р.С., Соколовский В.С., Волокитина Е.И., Степанов Н.Д., Жеребцов С.В., Алексеев Е.Б., Ночовная Н.А., Салищев Г.А. Структура и механические свойства сварных соединений из сплава на основе орторомбического алюминиды титана ВТИ-4, полученных импульсной лазерной сваркой // Известия высших учебных заведений. Цветная металлургия. 2023. Т. 29. № 2. С. 57–73. DOI: [10.17073/0021-3438-2023-2-57-73](https://doi.org/10.17073/0021-3438-2023-2-57-73).
15. Shengwei Zhang, Mingzhe Xi, Rui Liu, Mingyue Li, Xiaotian Guo, Yiming Gui, Jing Wu. Fabricating Ti–22Al–25Nb Intermetallic with Ductility Higher than 25% by Advanced Printing Technique: Point-Forging and Laser-Deposition // Materials Science and Engineering: A. 2022. Vol. 850. Article number 143520. DOI: [10.1016/j.msea.2022.143520](https://doi.org/10.1016/j.msea.2022.143520).
16. Xiaochong Sui, Guofeng Wang, Qing Liu, Yongkang Liu, Yuqing Chen. Fabricating Ti₂AlNb sheet with tensile strength higher than 1500 MPa by hot packed rolling spark-plasma-sintered pre-alloyed Ti the B2 + O phase field // Journal of Alloys and Compounds. 2021. Vol. 876. Article number 160110. DOI: [10.1016/j.jallcom.2021.160110](https://doi.org/10.1016/j.jallcom.2021.160110).
17. Yaran Zhang, Yongchang Liu, Liming Yu, Hongyan Liang, Yuan Huang, Zongqing Ma. Microstructures and tensile properties of Ti₂AlNb and Mo-modified Ti₂AlNb alloys fabricated by hot isostatic pressing // Materials Science and Engineering: A. 2020. Vol. 776. Article number 139043. DOI: [10.1016/j.msea.2020.139043](https://doi.org/10.1016/j.msea.2020.139043).

УДК 669.017.165

doi: <https://doi.org/10.18323/2782-4039-2026-1-75-8>

Влияние режимов термической обработки на структуру и механические свойства ковального сплава на основе орторомбического алюминиды титана ВТИ-4

Соколовский Виталий Сергеевич^{*1,3}, кандидат технических наук, научный сотрудник
лаборатории Объемных наноструктурных материалов

Наумов Станислав Валентинович^{1,4}, кандидат технических наук, старший научный сотрудник
лаборатории Объемных наноструктурных материалов

Панов Дмитрий Олегович^{1,5}, кандидат технических наук, старший научный сотрудник
лаборатории Объемных наноструктурных материалов

Лукьянов Василий Васильевич^{2,6}, кандидат технических наук,
начальник отдела сложнопрофильного формообразования

Салищев Геннадий Алексеевич^{1,7}, доктор технических наук, профессор,
заведующий лабораторией Объемных наноструктурных материалов

¹Белгородский государственный национальный исследовательский университет, Белгород (Россия)

²Научно-производственная ассоциация «Технопарк Авиационных Технологий», Уфа (Россия)

*E-mail: sokolovskiy@bsuedu.ru

³ORCID: <https://orcid.org/0000-0002-4363-3604>

⁴ORCID: <https://orcid.org/0000-0002-4084-8861>

⁵ORCID: <https://orcid.org/0000-0002-8971-1268>

⁶ORCID: <https://orcid.org/0009-0006-3621-3966>

⁷ORCID: <https://orcid.org/0000-0002-0815-3525>

Поступила в редакцию 09.09.2025

Пересмотрена 23.01.2026

Принята к публикации 19.02.2026

Аннотация: Проблема. В настоящее время в области исследования сплавов на основе орторомбического алюминиды Ti₂AlNb отсутствуют данные о связи режимов термической обработки, структурных параметров и механических ха-

рактических для обеспечения баланса прочности и пластичности. **Цель.** Установлении связи между режимами термической обработки, микроструктурными характеристиками (размеры О-фазы, объемная доля α_2 -фазы) и механическими характеристиками при комнатной температуре, а также определение режима термообработки, обеспечивающего наилучший баланс прочности и пластичности для сплава ВТИ-4. **Методы.** В работе был применен метод всесторонней изотермическойковки для формирования мелкозернистой глобулярной структуры с целью повышения пластических характеристик сплава. Последующую двухступенчатую термообработку проводили в $\alpha_2+\beta+O$ -фазовой области. Механические характеристики определены при испытаниях на растяжение. **Результаты.** Исследовано влияние температуры закалки и старения на размер и объемную долю частиц α_2 и О-фаз. Обоснован выбор режимов термической обработки, направленный на формирование структуры, обеспечивающий высокие прочностные и пластические свойства сплава ВТИ-4. Установлено, что при нагреве под закалку до $T=900\text{ }^\circ\text{C}$ сохраняются выделения О-фазы в тройных стыках по границам β -зерен; при последующем старении формируются частицы и прослойки О-фазы, толщина которых увеличивается с ростом температуры, что приводит к снижению прочности и пластичности. Установлено также, что нагрев под закалку из верхней части $\alpha_2+\beta+O$ -фазовой области ($T=960\text{ }^\circ\text{C}$) сохраняет глобулярную микроструктуру, приводя к растворению частиц О-фазы и, соответственно, насыщая легирующими элементами β -фазу. Повышение температуры закалки также снижает объемную долю частиц α_2 -фазы и предотвращает формирование прослоек О-фазы по границам β -зерен при старении в интервале температур $760\text{--}800\text{ }^\circ\text{C}$. **Выводы.** Исследование влияния температуры старения в интервале $760\text{--}840\text{ }^\circ\text{C}$ позволило установить, что чем ниже температура, тем меньше толщина частиц О-фазы, выше прочность и меньше пластичность. Определен оптимальный режим термической обработки: закалка $T=960\text{ }^\circ\text{C}$, $\tau=2\text{ ч}$ и старение $T=800\text{ }^\circ\text{C}$, $\tau=6\text{ ч}$. После такой термической обработки кованный сплав ВТИ-4 демонстрирует высокую прочность и пластичность ($\sigma_{0,2}=1180\text{ МПа}$, $\sigma_B=1300\text{ МПа}$, $\delta=6,2\text{ \%}$).

Ключевые слова: орторомбический алюминид титана Ti_2NbAl ; сплав ВТИ-4; всесторонняя изотермическаяковка; закалка; старение; механические свойства

Благодарности: Работа выполнена при финансовой поддержке Российского научного фонда (соглашение № 19-79-30066) с использованием оборудования Центра коллективного пользования «Технологии и материалы» НИУ «БелГУ», https://rscf.ru/prjcard_int?19-79-30066.

Статья подготовлена по материалам докладов участников XII Международной школы «Физическое материаловедение» (ШФМ-2025), Тольятти, 15–19 сентября 2025 года.

Для цитирования: Соколовский В.С., Наумов С.В., Панов Д.О., Лукьянов В.В., Салищев Г.А., Влияние режимов термической обработки на структуру и механические свойства кованого сплава на основе орторомбического алюминидатитана ВТИ-4 // Frontier Materials & Technologies. 2026. № 1. С. 97–106. DOI: <https://doi.org/10.18323/2782-4039-2026-1-75-8>.